



CONTROL OF CONTINUOUS RHEOCASTING PROCESS
USING HEAT FLOW MODEL

Abdel-Wahed M. Assar, Nahed A. El-Mahallawy,
Mohamed A. Taha and Ahmed S. El-Sabbagh

Dept. of Mechanical Design and Production Engineering,
Faculty of Engineering, Ain- Shams University
Abaseia, Cairo, Egypt

ABSTRACT:

In the continuous rheocasting process, a semi-solid alloy is obtained from the exit port of the apparatus at a given rate and with a given fraction solid. This fraction solid is dependent on the corresponding temperature within the solid-liquid range which should be controlled accurately by the process parameters for a given rheocaster stirring chamber.

For this purpose a heat flow model has been established for the continuous rheocasting of Bi-17wt%Sn alloy. The heat transfer calculations are based on the solution of the two-dimensional partial differential equations using a finite difference method. An excellent agreement between calculations and experimental results is found. Computations are carried out in order to find the influence of stirring chamber dimensions on the alloy exit temperature and therefore, the volume fraction solid. The influence of input metal temperature and metal flow rate on the exit temperature and volume fraction solid are also found.



INTRODUCTION:

During the last decade, considerable research work has been directed towards the improvement of alloy properties in the as cast condition by applying some innovative casting processes [1]. One of the processes which shows remarkable improvement in soundness, homogeneity and structure is the rheocasting (or stirr-casting) process. This process consists of vigorously agitating the alloy in the solid-liquid temperature range, to temperature between the liquidus and solidus. There are two techniques either batch type or continuous type rheocasting. The continuous type is more suitable for practice [3].

Many publications have appeared on the process studying slurry rheological behaviour and as-cast properties such as soundness, structure, homogeneity, mechanical properties and deformability [4-12]. These publications indicate many promising aspects of the process and as-cast properties produced. However, the application of the process on industrial scale is still very limited due to the difficulty in controlling the process parameters.

This paper is a part of a research program which tries to contribute in solving this problem. A heat transfer model, which gives the temperature gradient produced in Bi-17wt%Sn alloy contained inside a continuous rheocaster, is presented. The influence of rheocaster dimensions and other process variables on the temperature of the produced slurry is obtained.

Experimental Set up and procedure:-

Rheocasting:

The continuous rheocasting consists mainly of an upper cylindrical crucible made of austenitic cast-iron and a lower smaller cylindrical stirring chamber located on the same axis. The upper chamber (crucible) has 175 mm. internal diameter and 240 mm. height while the lower chamber (stirring chamber) has 39.6 mm. internal diameter and 200 mm. height. Four electrical resistance coils of 4 KW are used to heat the upper chamber. These coils are connected to a transformer with a built in temperature controller to regulate the temperature inside the chamber with ± 2 K. Additional resistance coils, used to heat the stirring chamber, are also connected to another transformer with a temperature controller. The temperature of the air gap existing between the coils and the stirring chamber was controlled between these coils and the stirring chamber was also controlled within ± 2 K. At the same time a cooling coil (copper tube) is installed around the stirring chamber and connected to a water bath with a digital temperature controller, where the temperature was



were used to produce an appropriate temperature gradient in the alloy along the axis of the stirring chamber. The value of the temperature gradient will determine the temperature and consequently the volume fraction solid at the exit port. Metal flow through this port was controlled by the vertical position of the stirrer, which is a stainless steel bar (35.6 mm. in diameter and 510 mm. long) with a hemispherical lower end. The lower part of the stirrer which is inserted in the stirring chamber has a special shape in order to get an efficient agitation action. The stirrer was powered by 1.8 KW, 3000 rpm D.C. motor connected to a speed control unit to achieve a constant speed with the variation of the torque. The alloy was solidified gradually during its downward flow in the stirring chamber while it is subjected to vigorous agitation provided by the stirrer. To prevent the freezing of the alloy below the exit port in the case of non-continuous flow, an additional resistance heater was placed at the exit port of the rheocaster to heat its vicinity to a temperature equals to the exit temperature of the slurry $\pm 5K$. Five Chromel-Alumel thermocouples were set in the wall of the stirring chamber along its height and were connected to five channel chart recorder.

Rheocasting experiments:-

Before starting the process, the charge in the upper and middle chamber was heated to a temperature about 40 K above the liquidus. After complete melting, the stirrer was set in motion at the desired speed. The power in the bottom coil was set on to keep the exit nozzle temperature at the appropriate level while that in the middle coil was set to keep the atmospheric temperature around the cooling coil at the appropriate level. Once the slurry temperature has reached the required level and consequently the desired volume of the solid fraction, the stainless steel stirrer was raised from the exit port and the slurry started flowing out. The flow rate was controlled by adjusting the position of the stirrer inside the stirring chamber. The amount of heat extracted from the stirring chamber was controlled by the input temperature of the cooling water and the temperature of the controlled furnace (consequently the atmospheric temperature around the cooling coil). Since the amount of heat was kept constant, therefore the volume fraction solid at the exit port of the stirring chamber will be inversely proportional to the flow rate and input temperature. During the flow of metal slurry in the stirring chamber, the input temperature is kept above the liquidus. Once the thermocouples readings indicate that steady state has been reached, the metal slurry was quenched in a cooled copper mould (4 gm.) with a cylindrical cavity (8mm. diameter, 8 mm. height).



Heat Flow Model:

In the continuous rheocasting process, the molten metal flows from the large chamber which consists of a reservoir, and enters the stirring chamber at a temperature 20K above the liquidus temperature figure 1. The stirring chamber is subjected to a radiative heat from the furnace, natural convection from the air present in the furnace - chamber gap, and to conductive cooling of the cooling coils, as shown in Fig. 1. At the bottom of the stirring chamber, a resistance furnace is present to keep the temperature of the atmosphere equal to the exit temperature of the slurry. As the melt flows downwards in the stirring chamber with a constant speed, steady state condition is reached and the process can be considered similar to the steady state continuous casting.

The heat transfer calculations are based on the solution of the two dimensional steady state partial differential equations given by:

$$K (d^2T/dz^2 + d^2T/dr^2 + (1/r)dT/dr) + q - C_p V(dT/dz) = 0$$

-----(1)

It is to be noted that:

- The term $K(d^2T/dz^2)$ corresponds to the variation of temperature parallel to the axis of the stirring chamber.
- The term $K(d^2T/dr^2 + (1/r)dT/dr)$ corresponds to the radial temperature variation.
- The term $C_p V (dT/dz)$ corresponds to the thermal capacity due to the longitudinal displacement of the slurry. Q corresponds to the evaluation of latent heat due to change in phase.

Assumptions:-

The assumptions used in the calculation are:

1. No heat flow between slurry and surrounding atmosphere at the exit port of the stirring chamber.
2. The temperature of the cooling water is taken as the average of the input and output temperature.
3. As the melt cools in the stirring chamber, heat flow will be only by conduction in both liquid and semi-solid state.
4. There is a heat flow resistance at metal/stirrer, metal/stirring chamber interfaces and between cooling coil and external wall of the stirring chamber. Values of the heat flow resistance are first assumed then adjusted according to experimental results.

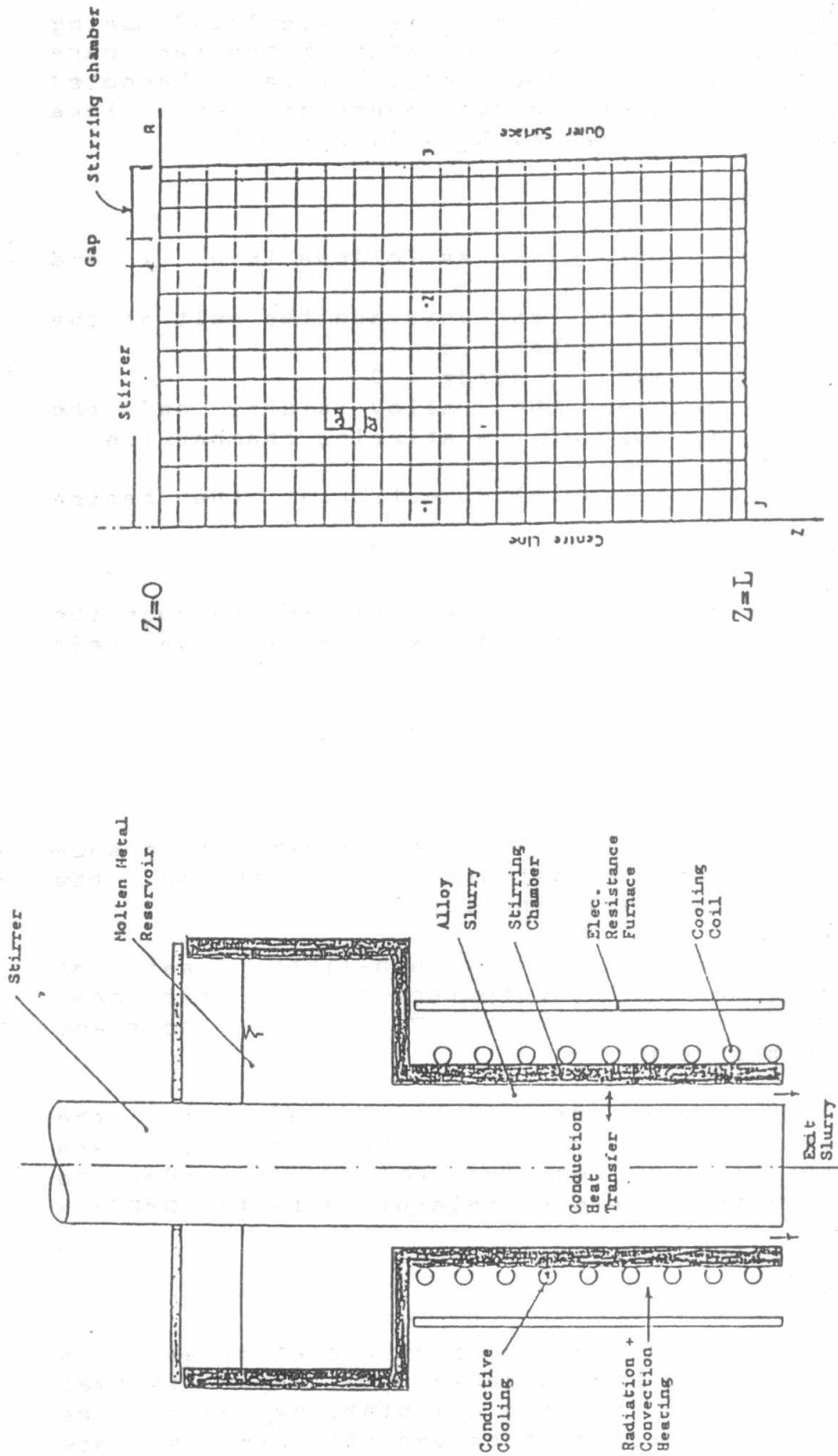


Fig. 2 The mesh points and their positions used in the computations.

Fig. 1 Schematic drawing of the stirring chamber with heating and cooling coil, showing heat flow



5. The thermal conductivity of the liquid metal K_1 and of the mixture of liquid plus solid K_m are calculated using the rule of linearity mixture using^m that of the two pure metals and the two phases respectively. It is to be noted that the conductivities of the two phases are very close to each other ($K_1 = 10.1$ W/m K, $K_m = 10.2$ W/m K).

Boundary Conditions:-

The boundary conditions are given as follows (Fig. 1 and 2):

a) No heat flow between the reservoir and the melt at the entrance of the stirring chamber i.e.

$$\text{at } z = 0 \quad T = T_1 \quad \text{and} \quad dT/dz = 0$$

b) No heat flow¹ between the alloy slurry and the atmosphere at the exit port of the stirring chamber i.e.:

$$\text{at } z = L \quad dT/dz = 0$$

c) No heat flow in the radial direction at the centre line of the stirrer i.e.:

$$\text{at } r = 0 \quad dT/dr = 0$$

d) The amount of heat flow in radial direction through the outer surface of stirring chamber is equal to the heat extracted by the cooling system i.e.:

$$\text{at } r = R_2 \quad , \quad dT/dr = Q \quad \text{and} \quad d^2T/dr^2 = 0$$

Method of solution:

In order to solve equation (1), the finite difference method is applied and a network is placed on the longitudinal section as shown in fig. 2.

In order to solve the highly non-linear set of differential equations by the computer, the radiation heat transfer term T^4 is replaced by T times a constant containing the other terms.

The set of linear equations will be solved using the Gauss-Seidel iterative method (13). The iteration were stoped when the error is less than 0.1 K. In order to speed up the iteration, an over relaxation factor OMEGA = 1.1 was used.

Thermal parameters:

The thermal and physical properties of the alloy used in the computations are given in table (1). Some thermal resistances are needed for the computations which are resistance between the copper tube and the outer surface of the stirring chamber ETA, the resistance between the alloy slurry and the inner surface of the stirring chamber

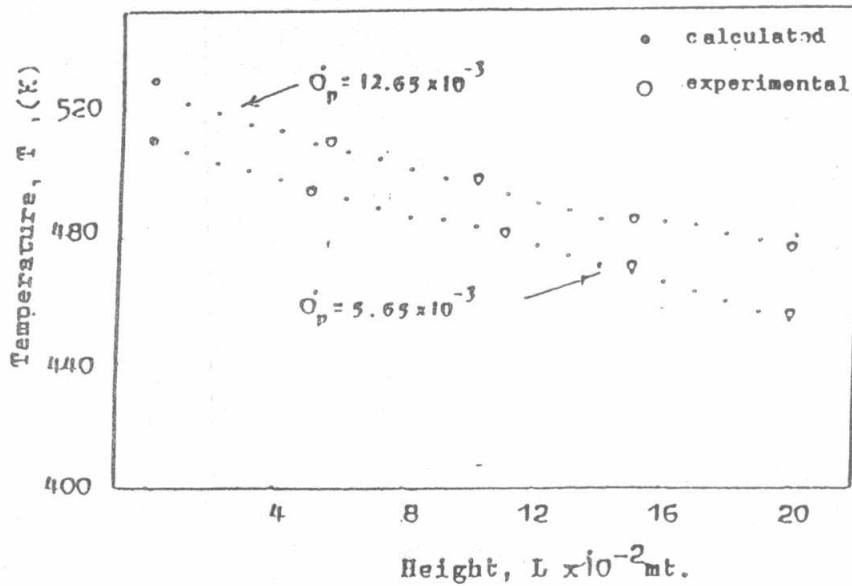


Fig. 3 Experimental and calculated temperature distribution of Bi-17%wt Sn slurry along the height of the stirring chamber at two values of flow rate of 5.65×10^{-3} and 12.65×10^{-3} Kg/s and shear rate of 270 1/s.

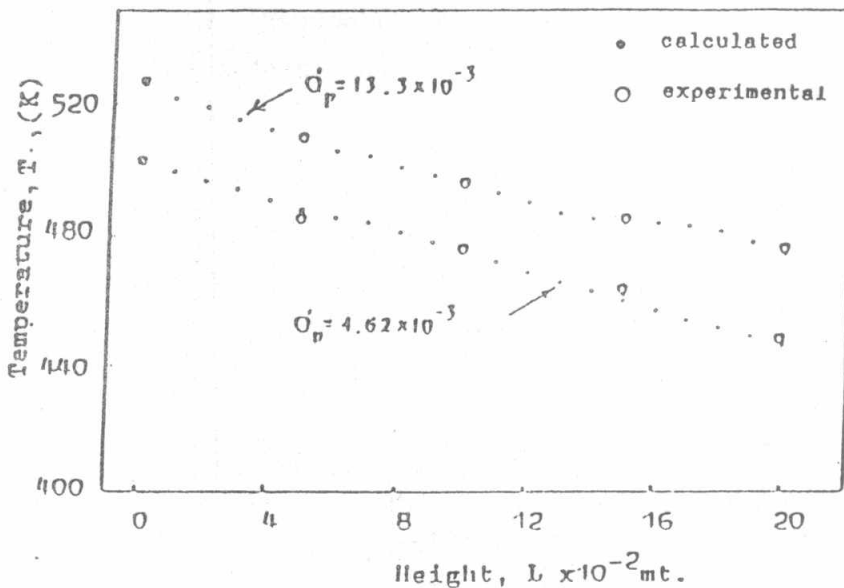


Fig. 4 Experimental and calculated temperature distribution of Bi-17%wt Sn slurry along the height of the stirring chamber at two values of flow rate of 4.62×10^{-3} and 13×10^{-3} Kg/s and shear rate of 450 1/s.

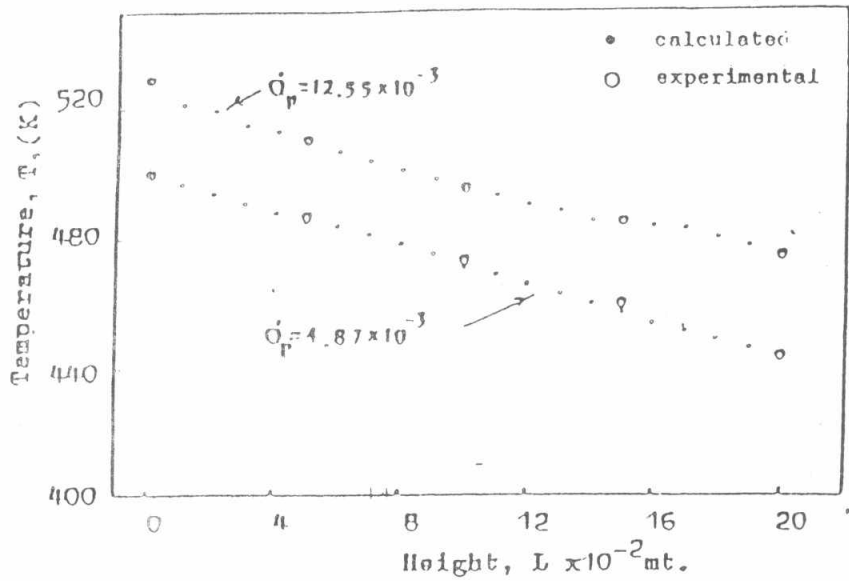


Fig.5 Experimental and calculated temperature distribution of Bi-17%wt Sn slurry along the height of the stirring chamber at two values of flow rate of 4.87×10^{-3} and 12.55×10^{-3} Kg/s and shear rate of 675 1/s.

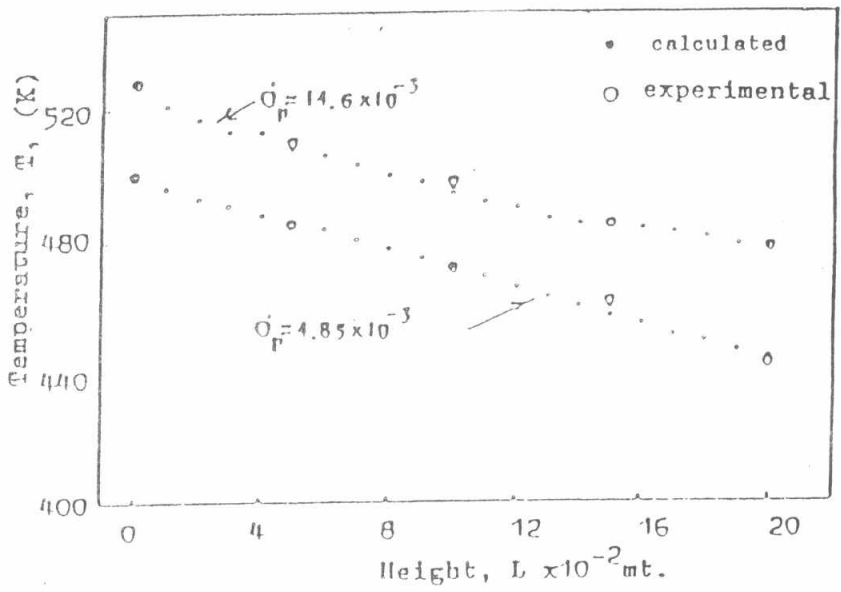


Fig. 6 Experimental and calculated temperature distribution of Bi-17%wt Sn slurry along the height of the stirring chamber at two values of flow rate of 4.85×10^{-3} and 14×10^{-3} Kg/s and shear rate of 900 1/s.



in terms of temperature distribution along the axis of the stirring chamber and the computed results for two different flow rates are presented in fig. 3 to 6. The best fitting between the experimental and computed results gave the following values of heat resistances:-

$$\text{ETA} = 1 \times 10^{-3} \text{ m}^2 \text{ K/W}, \quad \text{GAMA} = \text{PHI} = 0 \text{ m}^2 \text{ K/W}$$

Table (1): Physical properties of Bi-17/wt pct Sn alloy^[14]

Thermal conductivity of the liquid alloy	10.1 (W m ⁻¹ K ⁻¹)
For T in the range 486 - 573K	
Thermal conductivity of the solid alloy	10.2 (W m ⁻¹ K ⁻¹)
For T in the range 486 - 433K	
Density of the alloy	9.3x10 ³ (Kg m ⁻³)
Latent heat of fusion	39501 (J Kg ⁻¹)
Melting point	486 K
Specific heat	180.4 (J Kg ⁻¹ K ⁻¹)

EFFECT OF STIRRING CHAMBER DIMENSIONS ON EXIT TEMPERATURE:

The dimensions of the stirring chamber which have the main effect on the exit temperature and the corresponding volume of solid fraction are the height of the stirring chamber and the number of cooling coils per unit height of the stirring chamber. As the cooling rate is slow in the stirring chamber the solidification of the alloy is considered under equilibrium condition, and the phase distribution in the mushy zone can be calculated using the lever rule. The relation between the temperature, T and fraction solid, G_s is given by:-

$$G_s = 1 - 48.5 / (261.5 - T)$$

The effect of the height of the stirring chamber, L, on the exit temperature, T_{exit}, and the corresponding volume fraction solid, G_s is shown in fig. 7. At the same number of cooling coils per unit height, N_c = 50, flow rate, Q_g = 9 x 10⁻³ Kg/s and at different values of input temperatures, T_i, the exit temperature decreases with increasing the height, L. This result is reasonable since the amount of heat extracted from the outer surface of the stirring chamber increases with the height L. The effect of L on t_{exit} is more pronounced at lower T_i and at higher L values. For example at T_i = 500 K T_{exit} decreases from 478 to 447 K with increasing the height L from 8 x 10⁻³ to 20 x 10⁻³ mt., and at T_i = 5309 K, T_{exit} decreases from 482 to 472 K with increasing L from 8 x 10⁻³ to 20 x 10⁻³ mt.

The effect of the number of cooling coils per unit height, N_c

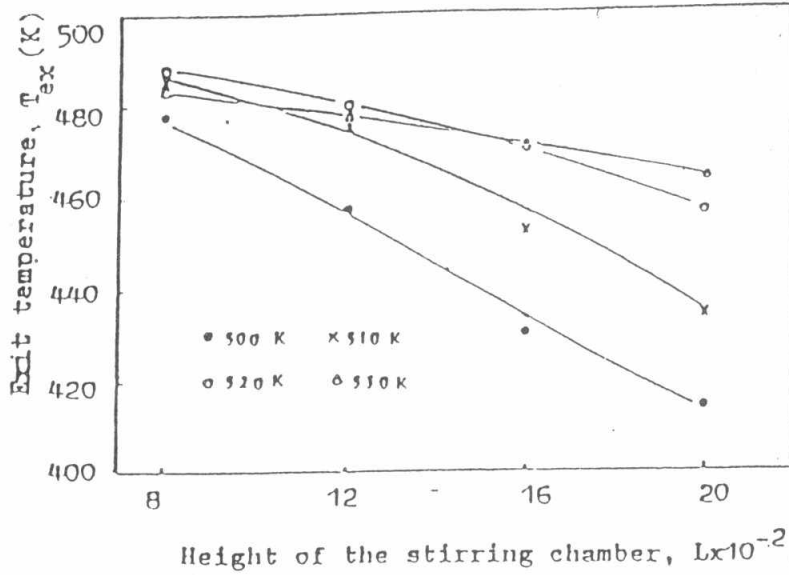


Fig. 7 Effect of height of the stirring chamber, L on T_{exit} at $N_g = 50$ 1/m and $Q_p = 9 \times 10^{-3}$ Kg/s and different values of T_1 of 500, 510, 520 and 530 K.

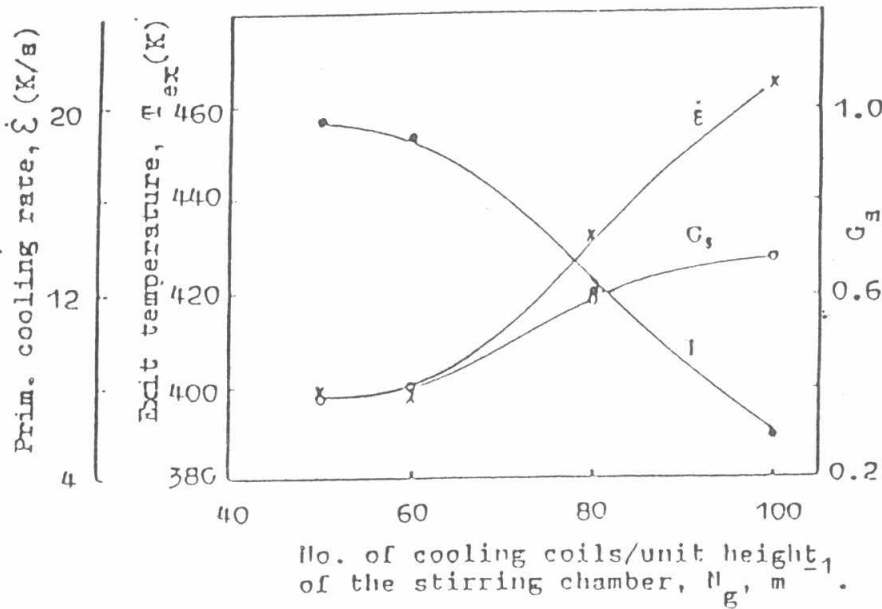


Fig. 8 Effect of no. of cooling coils/unit height of the stirring chamber N_g on \dot{C} , T_{exit} and G_s at $L = 0.2$ m, $Q_p = 9 \times 10^{-3}$ Kg/s and $T_1 = 510$ K.

is shown in fig. 8 . The exit temperature decreases with increasing N_g from 50 to 60 above which it decreases rapidly till 390 °K at $N_g = 100$. The corresponding solid fraction G_s at the exit port increased from 0.39 to 0.65 by increasing N_g from 50 to 100. As the primary cooling rate has the major effect on the structure of the rheocast material it is found that E increases from 8 to 21 K/s as N_g increases from 50 to 100. This behaviour is reasonable since at high T_{exit} T_i is small and as the flow rate is kept constant, the resulting cooling rate E will be lower. The values of E are plotted for different N_g in fig. 8 .

EFFECT OF INPUT TEMPERATURE AND METAL FLOW RATE ON THE EXIT TEMPERATURE AND THE CORRESPONDING SOLID FRACTION*

Fig. 9 shows the effect of input temperature T_i on the exit temperature, volume fraction solid and the primary cooling rate. Increasing T_i from 500 to 530 K leads to an almost similar T_{exit} from 447 to 472 K therefore a corresponding decrease in G_s from 0.44 to 0.22. Also, the cooling rate decreases from 9.1 to 3.55 K/s shows the effect of the metal flow rate, Q_p on T_{exit} , G_s and E .

Increasing of Q_p leads to increasing both T_{exit} and E and to decreasing G_s . From the figure it is observed that increasing Q_p from 1×10^{-3} to 13×10^{-3} Kg/s results in increasing of T_{exit} at different N_g values. It is clear that Q_p has a pronounced effect on T_{exit} at $N_g = 80$.

Conclusions

From the above results and discussions the following conclusions can be drawn:

The slurry exit temperature and corresponding G_s , is mainly affected by the melt input temperature T_i , and the number of cooling coils per unit height of the stirring chamber N_g . It is also affected by the slurry flow rate Q_p and the height of the stirring chamber L . The exit temperature increases with increasing T_i and Q_p , and decreasing N_g and L .

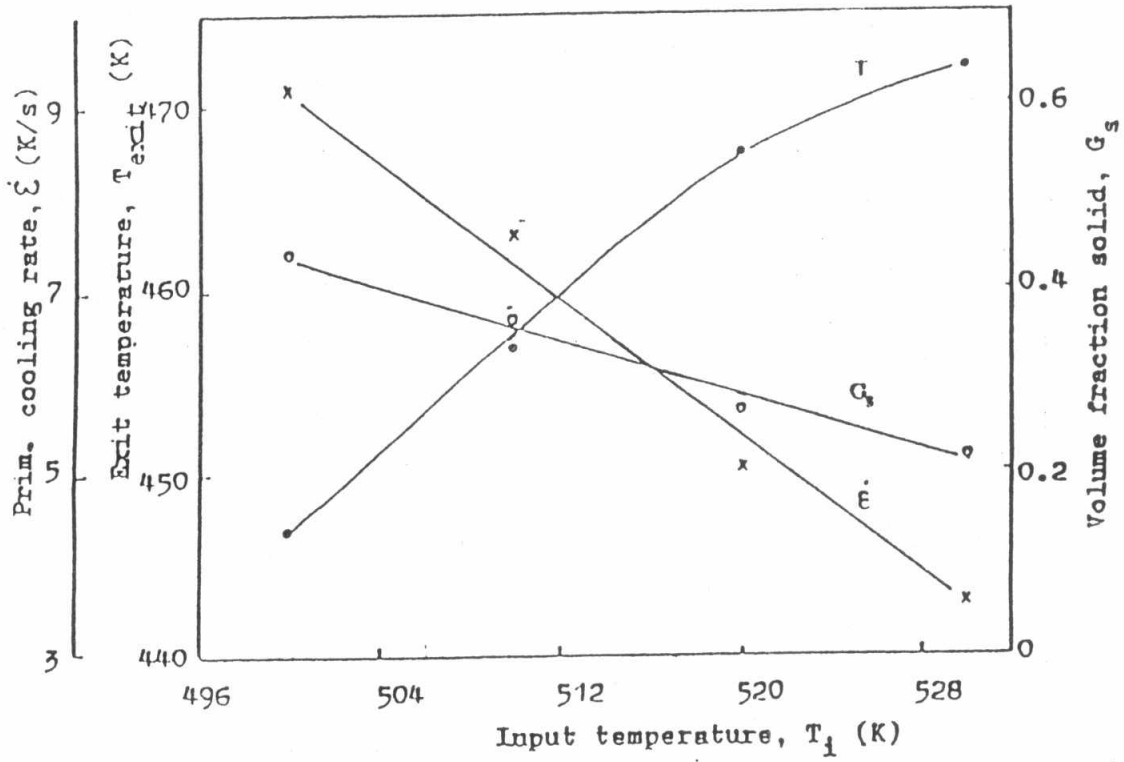


Fig. 9 Effect of input temperature T_1 on $\dot{\epsilon}$, T_{exit} and G_s at $L = 0.2$ m , $Q_p = 9 \times 10^{-3}$ Kg/s and $N_g = 50$ 1/m .

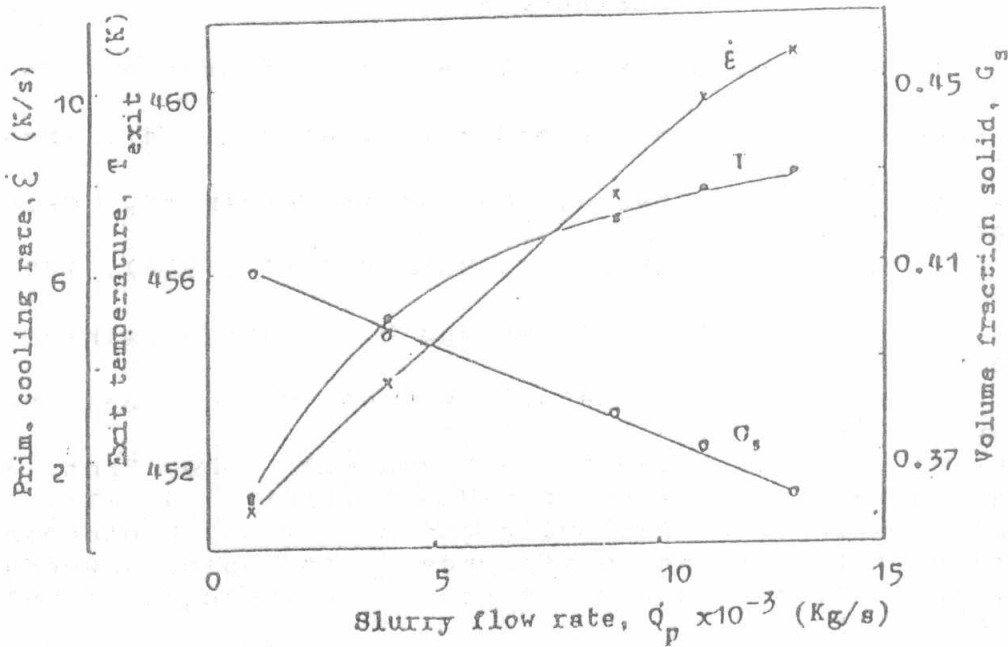


Fig. 10 Effect of slurry flow rate Q_p on E , T_{exit} and G_s at $L=0.2$ m, $T_i=510$ K and $N_g=50$ 1/m

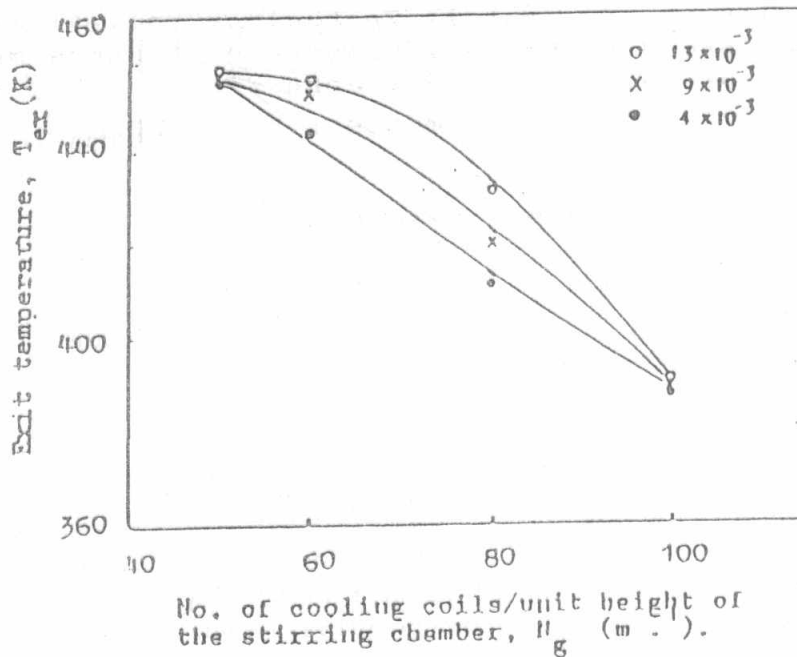


Fig. 11 Effect of N_g on T_{exit} at $L=0.2$ m and different values of Q_p of 13×10^{-3} , 9×10^{-3} and 4×10^{-3} Kg/s.



REFERENCES

1. N.A. El-Mahallawy and M.A. Taha, J. of Metals, Sept. (1985), 42 - 46.
2. D.B. Spencer, R. Mehrabian and M.C. Flemings. Met. Trans. 3, (1972), 1925 - 32.
3. A.M. Assar, Ph.D., Thesis, Ain Shams University, Cairo, Egypt (1985), 35 - 65.
4. P.A. Joly and R. Mehrabian, J. Mat. Sc. 11 (1976), 1393 - 1418.
5. A.M. Assar, N.A. El-Mahallawy and M.A. Taha, Aluminium 57 (1981) 807 - 810.
6. A.M. Assar, N.A. El-Mahallawy and M.A. Taha, Met. Technology, 9 (1982) 165 - 170.
7. A. El-Sawy, N.A. El-Mahallawy and M.A. Taha, Proc. 7th Int., Light Metal Congress (Leoben-Wien) (1981) 114 - 115.
8. N.A. El-Mahallawy, N. Fat-Halla and M.A. Taha, Proceedings of the fourth International Conference, Stockholm, Sweden, edited by J. Carlson and N.G. Ohlson, 15 - 19 August (1983), Vol. 23, 695 - 702.
9. M.A. Taha and N.A. El-Mahallawy, Proc. 3rd Int. Conf. on Mechanical behaviour of material, (ICM3), Cambridge, U.K. (1979) Vol. 2, 537.
10. M.C. Flemings and R. Mehrabian, ASM, Metal Park, Ohio, (1976) P. 98. P. 203 - 213.
11. M.A. Taha and N.A. El-Mahallawy, Advanced Technology of plasticity 1984, Vol. 1.
12. M.A. Taha and M. Suery, Metals Technology Vol. 11 (1984).
13. G.E. Forsythe and W.R. Warsow, "Finite difference methods for partial differential equations", John Wiley, N.Y., 1959.
14. Thermophysical properties of matter, Vol.4 pp.22 , Vol.1 pp. 511.

=====